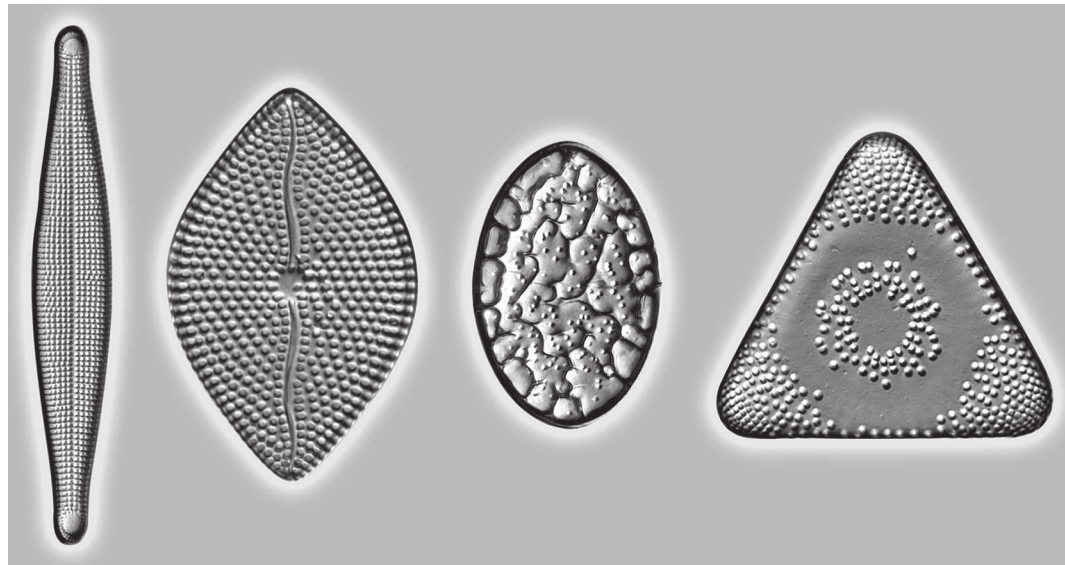


Nova Hedwigia

Beiheft 152

Jakub Witkowski

Early Paleocene-Late Eocene diatoms from the Blake Nose, western North Atlantic Ocean



J. Cramer

in Borntraeger Science Publishers · Stuttgart · 2022

Nova Hedwigia

Beiheft 152

Early Paleocene-Late Eocene diatoms from the Blake Nose, western North Atlantic Ocean

Jakub Witkowski

With 2 figures, 156 plates and 7 tables



J. Cramer
in Borntraeger Science Publishers · Stuttgart · 2022

Witkowski, J.: Early Paleocene-Late Eocene diatoms from the Blake Nose, western North Atlantic Ocean (Nova Hedwiga, Beiheft 152)

Author's address:

Institute of Marine and Environmental Sciences, University of Szczecin, ul. Mickiewicza 18,
70-383 Szczecin, Poland
e-mail: jakub.witkowski@usz.edu.pl

We appreciate suggestions and comments on this book to editors@schweizerbart.de

ISBN 978-3-443-51077-0

ISBN ebook (epdf) 978-3-443-51078-7

ISSN 1438-9134 (Nova Hedwigia, Beiheft)

Information on this title: **www.borntraeger-cramer.com/9783443510770**

© 2022 Gebr. Borntraeger Verlagsbuchhandlung, Stuttgart

All rights reserved including translation into foreign languages. This book or parts thereof may not be reproduced, digitalized or stored in any form without permission of the publishers.

Publisher: J. Cramer in der

Gebr. Borntraeger Verlagsbuchhandlung
Johannesstr. 3A
70176 Stuttgart, Germany
mail@borntraeger-cramer.de
www.borntraeger-cramer.de

♾ Printed on permanent paper conforming to ISO 9706-1994

Printed in Germany by Esser printSolutions GmbH, Bretten

Contents

Abstract	1
Introduction.....	1
Materials and methods	4
Taxonomic Part	12
List of Taxa	12
I. <i>ABAS</i> Ross & Sims (1980)	15
II. <i>ACTINOPTYCHUS</i> Ehrenberg (1843)	21
III. <i>AMPHORA</i> Ehrenberg ex Kützing (1844)	33
IV. <i>ANÄULUS</i> Ehrenberg (1844a)	37
V. <i>ANUOPLICATA</i> (Gleser) Gleser in Gleser et al. (1992).....	41
VI. <i>ARACHNOIDISCUS</i> Deane ex Shadboldt (1852)	44
VII. <i>AULISCUS</i> Ehrenberg (1843)	49
VIII. <i>BIDDULPHIA</i> Gray (1821)	51
IX. <i>BRIGGERA</i> Ross & Sims (1985)	55
X. <i>BRIGHTWELLIA</i> Ralfs in Pritchard (1861).....	60
XI. <i>CLAVICULA</i> Pantocsek (1886)	67
XII. <i>CORTINOCORNUS</i> Gleser (1984)	71
XIII. <i>COSCINODISCUS</i> Ehrenberg (1839a)	75
XIV. <i>CRASPEDODISCUS</i> Ehrenberg (1844b)	79
XV. <i>CRASPEDOPORUS</i> Greville (1863b)	85
XVI. <i>CYLINDROSPIRA</i> Mitlehner (1995)	87
XVII. <i>CYMATOSIRACEAE</i> Hasle, von Stosch & Syvertsen (1983)	88
XVIII. <i>DETTONIA</i> Frenguelli (1949)	91
XIX. <i>DEXTRADONATOR</i> Ross in Ross & Sims (1980)	96
XX. <i>DISTEPHANOSIRA</i> Gleser in Gleser et al. (1992)	103
XXI. <i>DREPANOPODHECA</i> Schrader ex Round et al. (1990)	109
XXII. <i>ENTOGONIA</i> Greville (1863c)	112
XXIII. <i>ENTOGONIOPSIS</i> Sims, Strelnikova, Witkowski & Williams in Witkowski et al. (2015)	112
XXIV. <i>EUNOTOGRAMMA</i> Weisse (1854)	123
XXV. <i>EUODIELLA</i> Sims (2000)	129

XXVI. <i>EUROSSIA</i> Sims in Mahood et al. (1993)	133
XXVII. <i>FENNERIA</i> Witkowski (2018)	135
XXVIII. <i>GRAMMATOPHORA</i> Ehrenberg (1840)	149
XXIX. <i>GRUNOWIELLA</i> Van Heurck (1896)	150
XXX. <i>HEMIAULUS</i> Heiberg (1863)	152
XXXI. <i>JOUSEA</i> Gleser (1967)	199
XXXII. <i>KTENODISCUS</i> Pantocsek (1889)	201
XXXIII. <i>LIRADISCUS</i> Greville (1865a)	207
XXXIV. <i>MASTOGLOIA</i> Thwaites in Smith (1856).....	213
XXXV. <i>MEDLINIA</i> Sims (1998)	219
XXXVI. <i>PEPONIA</i> Greville (1863b)	235
XXXVII. <i>PLAGIOTRICHIA</i> Greville (1859)	239
XXXVIII. <i>PORPEIA</i> Bailey ex Ralfs in Pritchard (1861)	243
XXXIX. <i>PROBOSCIA</i> Sundström (1986)	247
XL. <i>PSAMMODISCUS</i> Round & Mann (1986)	254
XLI. <i>PSEUDOPODOSIRA</i> Jousé in Proschkina-Lavrenko (1949).....	258
XLII. <i>PYRGUPYXIS</i> Hendey (1969)	269
XLIII. <i>QUADROCISTELLA</i> Suto (2006)	276
XLIV. <i>RHAPHONEIS</i> Ehrenberg (1844a)	281
XLV. <i>RHIZOSOLENIA</i> Brightwell (1858)	285
XLVI. <i>RUTILARIA</i> Greville (1863c)	287
XLVII. <i>SEXTIPUTEUS</i> Ross & Sims (2000).....	292
XLVIII. <i>SHESHUKOVIA</i> Gleser (1975)	293
XLIX. <i>SOLIUM</i> Heiberg (1863)	297
L. <i>STICTODISCUS</i> Greville (1861a)	299
LI. <i>STRANGULONEMA</i> Greville (1865c)	303
LII. <i>THAUMATONEMA</i> Greville (1863b)	307
LIII. <i>TOXARIUM</i> Bailey (1854)	309
LIV. <i>TRICERATIUM</i> Ehrenberg (1839b)	311
LV. <i>TRINACRIA</i> Heiberg (1863)	329
LVI. <i>TROCHOSIRA</i> Kitton (1870)	347
LVII. <i>TROSSULUS</i> Ross & Sims (2002)	351
LVIII. <i>VALLODISCUS</i> Suto (2005)	353
LIX. <i>XANTHIOISTHMUS</i> Suto (2006)	355
LX. <i>XANTHIOPYXIS</i> Ehrenberg (1844b)	357

Discussion	360
Acknowledgements	362
References	363

Abstract

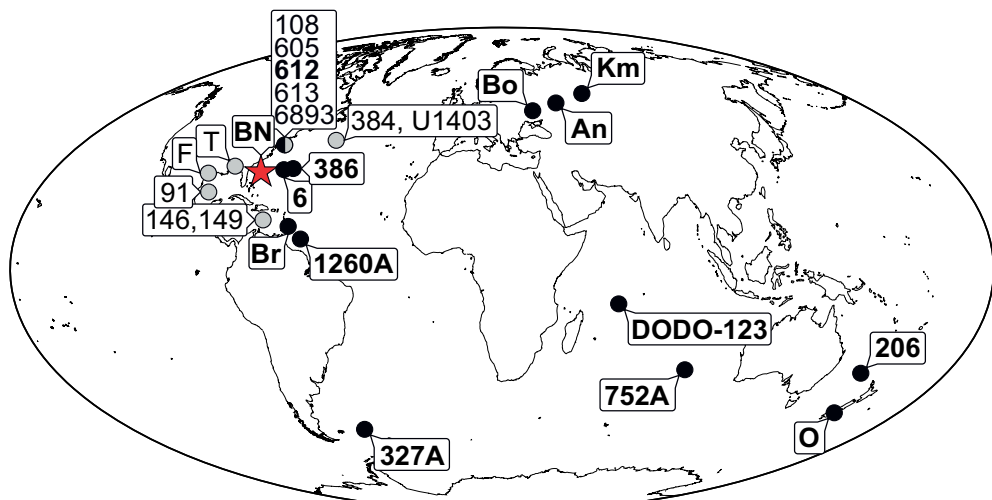
The Blake Nose area (western North Atlantic) represents the longest currently available single-locality record of diatom evolution, spanning approximately 30 million years of the early Cenozoic Era. This study provides a detailed taxonomic account of the diatom assemblages found in the lower Paleocene through upper Eocene deep-sea sediments recovered by Ocean Drilling Program Leg 171B from the Blake Nose. The main study sites are Holes 1050A, 1050C and 1051A. For comparative purposes, materials from other deep-sea holes and onshore sites are included as well. A total of 137 taxa representing 60 genera are examined using scanning electron and/or light microscopy. Two new combinations are performed (*Psammodiscus praenitidus* (Fenner) J. Witkowski, n. comb. and *Sheshukovia castellifera* (Grunow) J. Witkowski, n. comb.), and ten species are proposed as new (*Brightwellia plana* J. Witkowski, n. sp.; *Detonia wadeae* J. Witkowski, n. sp.; *Distephanosira gleichiae* J. Witkowski, n. sp.; *Euodiella beatae* J. Witkowski, n. sp.; *Hemiaulus curvaturoides* J. Witkowski, n. sp.; *Hemiaulus imperator* J. Witkowski, n. sp.; *Hemiaulus jordani* J. Witkowski, n. sp.; *Hemiaulus oreshkinae* J. Witkowski, n. sp.; *Medlinia? subtriangularis* J. Witkowski & P.A. Sims, n. sp.; and *Triceratium harwoodii* J. Witkowski, n. sp.). Emphasis in this study is on stratigraphic and geographic distribution of the diatom taxa encountered in the Blake Nose cores, and on documenting their morphological variability. The overall aim of this work is to provide a reference for future biostratigraphic and paleoceanographic studies involving early Paleogene marine diatoms.

Keywords: fossil diatoms; Paleocene; Eocene; Blake Nose; Atlantic Ocean; taxonomy; ODP Site 1050; ODP Site 1051

Introduction

Ever since the onset of scientific deep-sea drilling in the late 1960s, the western North Atlantic has been viewed as the key locus of biogenic silica accumulation through the early Paleogene period (i.e., Paleocene and Eocene, ~66 through 34 million years ago) characterized by greenhouse climates (Barron et al. 2015; Witkowski et al. 2020b, 2021). To date, well-preserved early Paleogene diatoms have been recovered in the Caribbean (e.g., Deep Sea Drilling Project [DSDP] Sites 91, 146/149 – see Fenner 1984a, 1985), the Blake Nose region (e.g., DSDP Site 390; Ocean Drilling Program [ODP] Sites 1049–1053 – see Gombos 1982; Fenner 1984a, 1985; Witkowski et al. 2020a, b), Bermuda Rise (DSDP Sites 6, 386 – Ross & Sims 2000; Bukry 1978a), J-Anomaly Ridge (DSDP Site 384 – Bukry 1978a, Integrated Ocean Drilling Program [IODP] Site U1403 – Hollis 2012), and from the North American continental slope off New Jersey and Delaware (DSDP Sites 108, 605, 612–613; Fenner 1984a, 1985; Abbott 1987; Gombos 1987; see also U.S. Geological Survey Diatom Locality 6893 – Andrews 1986, 1989) (Text-Fig. 1). There is also evidence from onshore sites (Text-Fig. 1), suggesting widespread deposition of early Paleogene diatom-rich sediments on the North American shelf (Laws & Thayer 1992; Davis et al. 2016; Witkowski et al. 2020b). The Blake Nose region (Text-Fig. 1), however, is unique among early Cenozoic diatom-bearing localities globally in that it represents the longest currently available record of diatom evolution through the Paleogene, spanning approximately 30 million years from the late early Paleocene to early late Eocene (Text-Fig. 2).

As briefly discussed in Witkowski et al. (2020a), comparatively few diatomists have participated in deep-sea drilling expeditions from the late 1990s on. As a consequence, few taxonomic papers on Paleogene diatoms from deep-sea sites have been published in recent decades, and the most recent monographic treatments are those from the 1970s-1980s, for instance: Fenner (1984a, 1985), Gombos (1982, 1987). Since then, many revisions have been made to diatom taxonomy, with numerous new genera proposed, and previously established taxa re-examined or redefined.

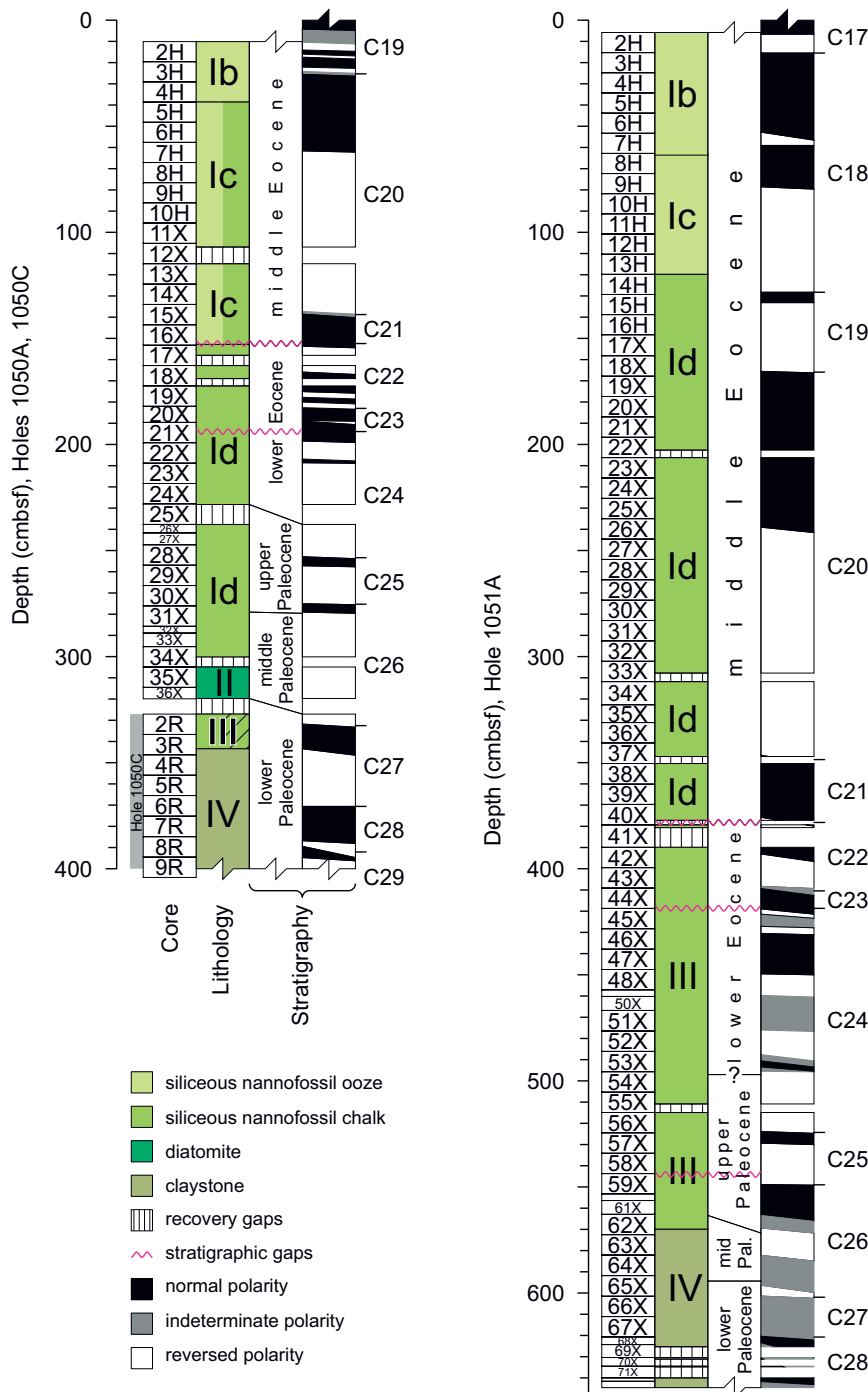


Text-Fig. 1: Study site location. The Blake Nose area is indicated with a star. Deep-sea and onshore sites examined for comparative purposes are indicated with black circles and labelled with bold font face. Prominent western North Atlantic diatom-bearing sites (including interpreted onshore locations) not examined in the present study are indicated with grey circles and labelled with normal font face. Abbreviations: BN – Blake nose; 6893 – core P-36(I) (U.S. Geological Survey Diatom Locality #6893); An – Ananino; Bo – Boromlya; Br – Barbados; F – Fayette County, Texas; Km – Kamyshlov; O – Oamaru; T – Tallahatta Formation outcrops in Alabama. Base map generated using the online Ocean Drilling Stratigraphic Network Advanced Plate Tectonic Reconstruction tool (www.odsn.de).

These new developments, however, remain largely scattered, and a synthesis is lacking.

The purpose of this work is to provide a concise and up to date taxonomic account of the Blake Nose early Paleogene diatom assemblages. As such, it is designed as a companion paper to two recent publications: Witkowski et al. (2020a and 2020b), but even more importantly, as a reference for future paleoceanographic and biostratigraphic work in the western North Atlantic. To this end, for each taxon included, this work provides:

1. A description, based on scanning electron microscope (SEM) and/or light microscope (LM) examination; for those taxa that could not be examined in SEM for this work, a citation is provided to relevant publications that do include SEM micrographs of the taxon in question. In several cases, usually of extremely rare and poorly known taxa, the description is based entirely on LM examination.
2. An indication of stratigraphic occurrence in the Blake Nose cores, including reference to magnetostratigraphy (Text-Fig. 2). This is based on the age models for Sites 1050 and 1051 developed in Witkowski et al. (2020a). Sub-bottom depths are reported for the intervals over which any given species was observed, expressed as ‘compacted meters below sea floor’ (cmbsf), ‘meters below sea floor’ (mbsf) or ‘meters composite depth’ (mcd), depending on the stratigraphic convention used in the relevant sources.
3. A discussion of any possible complications to the pattern of stratigraphic occurrences, for instance, downworking, reworking, laboratory contamination, known diachroneity, etc. The discussion also concerns any taxonomic issues that were found during the present study, or were discussed by previous authors. Finally, the range of morphological variability displayed by a given species is also discussed.
4. Wherever possible, a list of geographic distribution is compiled, along with published stratigraphic data.



Text-Fig. 2: Ocean Drilling Program Hole 1050A, 1050C and 1051A core recovery, lithology, and stratigraphy. Roman numerals refer to lithological units, as defined in the relevant site chapters (Norris, Kroon et al. 1998b-c). For details of study site stratigraphy, see Witkowski et al. (2020a). Abbreviations: cmbsf – compacted meters below sea floor; mid Pal. – middle Paleocene.

The astonishing taxonomic richness of the Blake Nose diatom assemblages makes it impossible to provide a detailed description based on SEM examination for each of the several hundred diatom taxa recorded in previous works. The following strategy has therefore been adopted in this work. For those taxa that have been documented in detailed monographic papers by other workers, the relevant works are cited, and – if that is the case – supplemented by citations to occurrence records that were published subsequent to the taxonomic account. For those taxa that were not yet subject to a closer scrutiny, a description is provided with as high accuracy as possible: based either on SEM or LM examination – or both. A number of taxa are here identified as specific morphotypes, but not yet formally proposed as new species or varieties. Hopefully, these loose threads will be followed and supplemented by future workers. Note that the most problematic taxa (i.e., *Paralia* and *Stephanopyxis*) are deliberately left out from this work, and will be examined in detail in future monographic publications.

Materials and methods

This work is based primarily on an extensive survey of deep-sea cores from ODP Holes 1050A, 1050C and 1051A drilled on the Blake Nose in the western North Atlantic (Text-Figs 1–2; Table 1), but materials from a number of additional deep-sea and onshore sites were also examined for comparative purposes (Table 1). Samples examined in SEM are listed in Table 2. Slides examined for this study are kept at the following repositories: Institute of Marine and Environmental Sciences, University of Szczecin (SZCZ), International Ocean Discovery Program Micropaleontological Reference Center (University of Nebraska-Lincoln; abbreviated as MRC), The Natural History Museum, London (abbreviated as BM). All slides examined for this study are tabulated in Tables 3–7.

Table 1. Deep-sea and onshore sites examined for this study, both as primary materials, and for comparative purposes, along with examination method and references. Abbreviations: Coords – geographic coordinates; SEM – scanning electron microscope; LM – light microscope.

Leg	Site	Hole	Region	Coords	Examined using	Comments	References
<i>Primary study sites:</i>							
171B	1050	A, C	Blake Nose, western North Atlantic	30.10°N 76.24°W	SEM, LM	Details in Tables 2–5	Norris, Kroon, et al. (1998b); Witkowski et al. (2020a)
171B	1051	A	Blake Nose, western North Atlantic	30.05°N 76.36°W	SEM, LM	Details in Tables 2–4	Norris, Kroon, et al. (1998c); Witkowski et al. (2020a)
<i>Materials from deep-sea sites examined for comparative purposes:</i>							
1	6	—	Bermuda Rise, western North Atlantic	30.84°N 67.65°W	SEM, LM	Details in Tables 2 and 6	Ewing, Worzel et al. (1969)
21	206	—	New Caledonia Basin, Southwest Pacific	32.01°S 165.45°E	LM	Details in Table 6	Burns, Andrews et al. (1973)
36	327	A	Falkland Plateau, South Atlantic	50.87°S 46.78°W	SEM	Details in Table 2	Barker, Dalziel et al. (1977)
43	386	—	Central Bermuda Rise, western North Atlantic	31.19°N 64.25°W	SEM, LM	Details in Tables 2 and 6	Tucholke, Vogt et al. (1979)
95	612	—	New Jersey continental slope, western North Atlantic	38.82°N 72.77°W	SEM, LM	Details in Tables 2 and 6	Poag, Watts et al. (1987)
121	752	A	Broken Ridge, tropical Indian Ocean	30.89°S 93.58°E	SEM	Details in Table 2	Peirce, Weissel et al. (1989)

171B	1053	A	Blake Nose, western North Atlantic	29.99°N 76.52°W	LM	Details in Table 5	Norris, Kroon, et al. (1998d)
207	1260	A	Ceara Rise, tropical western Atlantic	9.25°N 54.32°W	SEM	Details in Table 2	Erbacher, Mosher et al. (2004); Renaudie et al. (2010)
D1-DODO-123 dredging			Mascarene Plateau, Indian Ocean	10.42°S 63.25°E	LM	Details in Table 7	Ross & Sims (1980); Hennedy & Sims (1984)
<i>Materials from onshore sites examined for comparative purposes:</i>							
Ananino, Ulyanovsk District, Russia				53.40°N 47.30°E	SEM, LM	Details in Tables 2 and 7	Ross & Sims (1985)
Barbados				13.23°N 59.54°W	LM	Details in Table 7	Ross (1995); Witkowski et al. (2015)
Boromlya, Sumy District, Ukraine				50.62°N 34.97°E	SEM	Details in Table 2	Witkowski et al. (2012a)
Kamyshlov, Sverdlovsk District, Russia				56.90°N 62.70°E	SEM, LM	Details in Tables 2 and 7	Ross & Sims (1985); Witkowski et al. (2015)
Oamaru, Otago, New Zealand				45.10°S 170.95°E	SEM, LM	Details in Tables 2 and 7	Witkowski et al. (2017)

Table 2. List of materials examined using scanning electron microscope. Abbreviations: H – Hole; C – Core; T – Core type; Sc – Core-section; Int. – Interval; Bot. – Bottom; CAS – California Academy of Sciences; AWI – Alfred-Wegener-Institut; VSEGEI – All-Russian Geological Research Institute.

Leg	Site	H	C	T	Sc	Int. top [cm]	Int. bot. [cm]	Comments
<i>Materials from primary study sites:</i>								
171B	1050	A	3	H	6	100	101	—
171B	1050	A	5	H	1	100	101	—
171B	1050	A	14	X	1	100	101	—
171B	1050	A	16	X	2	100	101	—
171B	1050	A	17	X	2	100	101	—
171B	1050	A	21	X	2	100	101	—
171B	1050	A	27	X	1	70	71	—
171B	1050	A	28	X	1	90	91	—
171B	1050	A	29	X	1	91	92	—
171B	1050	A	30	X	1	100	101	—
171B	1050	B	13	X	3	10	11	—
171B	1050	C	2	R	5	100	101	—
171B	1051	A	10	H	1	36	37	—
171B	1051	A	36	X	1	50	51	—
171B	1051	A	42	X	1	50	51	—
171B	1051	B	8	H	5	5	6	—
<i>Materials from deep-sea sites examined for comparative purposes:</i>								
1	6	—	3	R	3	87	93	Material obtained from the A.L. Brigger Collection at CAS (accession no. 610596)
1	6	—	4	R	1	57	63	Material obtained from the A.L. Brigger Collection at CAS (accession no. 610598)
36	327	A	5	R	1	45	46	—
43	386	—	15	R	3	62	63	—
95	612	—	24	X	2	50	51	—
121	752	A	14	X	3	63	65	—

207	1260	A	12	R	4	36	37	—
<i>Materials from onshore sites examined for comparative purposes:</i>								
Ananino, Ulyanovsk District, Russia								Split of S.I. Gleser material obtained from VSEGEI
Boromlya, Sumy District, Ukraine								A.P. Jousé sample suite sample number 37
Kamyshlov, Sverdlovsk District, Russia								F. Hustedt Collection (AWI) accession no. E1685
Oamaru, Otago, New Zealand								F. Hustedt Collection (AWI) accession no. AT07

Table 3. SZCZ slides of Blake Nose materials prepared specifically for this study. Abbreviations: SZCZ – Institute of Marine and Environmental Sciences, University of Szczecin, Diatom Collection; H – Hole; C – Core; T – Core type; Sc – Core-section; Int. – Interval; Bot. – Bottom; MRC – International Ocean Discovery Program Micropaleontological Reference Center.

SZCZ Slide	Leg	Site	H	C	T	Sc	Int. top [cm]	Int. bot. [cm]	Fraction	Comment
27580	171B	1050	A	14	X	2	100	101	25-38 µm	holotypes of <i>Brightwellia plana</i> , <i>Medlinia? subtriangularis</i>
27581	171B	1050	A	3	H	6	33	34	>25 µm	donated to SZCZ by MRC; holotypes of <i>Detonia wadeae</i> , <i>Euodiella beatae</i>
27582	171B	1050	A	8	H	1	100	101	25-38 µm	holotypes of <i>Distephanosira gleichiae</i> , <i>Hemiaulus imperator</i>
27583	171B	1050	A	21	X	2	100	101	38-63 µm	holotype of <i>Hemiaulus curvatuloides</i>
27584	171B	1051	B	56	X	1	50	51	>25 µm	holotype of <i>Hemiaulus jordani</i>
27586	171B	1050	A	3	H	6	100	101	25-38 µm	holotype of <i>Triceratium harwoodii</i>
27825C	171B	1051	B	7	H	6	125	126	>25 µm	—
27830A	171B	1050	A	3	H	6	100	101	25-38 µm	—
27830C									25-38 µm	—
27830D									25-38 µm	—
27831A									38-63 µm	—
27831B									38-63 µm	—
27831C									38-63 µm	—
27831D									38-63 µm	—
27832A									63-100 µm	—
27832B									63-100 µm	—
27832C									63-100 µm	—
27833A	171B	1050	C	2	R	5	100	101	25-38 µm	—
27833B									25-38 µm	—
27833C									25-38 µm	—
27834A									63-100 µm	—
27834B									63-100 µm	—
27834E									63-100 µm	—
27835A	171B	1050	A	29	X	1	91	92	36-63 µm	—
27837A	171B	1050	A	27	X	1	70	71	38-63 µm	—
27838A	171B	1050	A	29	X	1	91	92	25-38	—
27839C	171B	1050	C	2	R	5	100	101	>25 µm	—
27839D									>25 µm	—
27840A	171B	1051	A	45	X	4	50	51	>25 µm	—
27842A	171B	1050	A	21	X	2	100	101	25-38 µm	—
27842B									25-38 µm	—
27843B									38-63 µm	—
27844A	171B	1050	A	21	X	1	100	101	38-63 µm	—

27845A	171B	1051	A	50	X	3	50	51	>25 µm	—
27846A	171B	1050	A	3	H	6	100	101	>25 µm	—
27846D	171B	1050	A	3	H	6	100	101	>25 µm	—
27847A	171B	1050	A	17	X	2	100	101	38-63 µm	—
27847B	171B	1050	A	17	X	2	100	101	38-63 µm	—
27848A	171B	1050	A	8	H	1	100	101	38-63 µm	—
27852A	171B	1050	A	14	X	1	100	101	38-63 µm	—
27853A	171B	1051	A	36	X	1	50	51	>25 µm	—
27853B	171B	1051	A	36	X	1	50	51	>25 µm	—
27854D	171B	1050	A	42	X	1	50	51	>25 µm	—
27855A									25-38 µm	—
27856B	171B	1050	A	30	X	1	100	101	38-63 µm	—
27857A									63-100 µm	—
27859B	171B	1051	A	46	X	1	50	51	>25 µm	—
27860B	171B	1050	A	21	X	1	100	101	63-100 µm	—
27861B	171B	1050	A	14	X	1	100	101	25-38 µm	—
27862B	171B	1050	A	8	H	1	100	101	25-38 µm	—

Table 4. SZCZ slides of Blake Nose materials prepared for previous studies. Abbreviations: SZCZ – Institute of Marine and Environmental Sciences, University of Szczecin, Diatom Collection; Int. – interval; Bot. – bottom.

SZCZ slide	Leg	Site	Hole	Core	Type	Section	Int. top [cm]	Int. bot. [cm]
<i>Slides prepared for Witkowski et al. (2014) study:</i>								
16093b	171B	1051	B	9	H	1	36	37
16105b	171B	1051	B	9	H	2	6	7
16113c	171B	1051	B	9	H	2	87	88
17090d	171B	1051	A	8	H	1	6	7
17091b	171B	1051	A	8	H	1	16	17
17092d	171B	1051	A	8	H	1	26	27
17093c	171B	1051	A	8	H	2	6	7
17095a	171B	1051	A	8	H	2	66	67
17095d	171B	1051	A	8	H	2	66	67
17096c	171B	1051	A	8	H	2	96	97
17098d	171B	1051	A	9	H	1	6	7
17099c	171B	1051	A	9	H	1	36	37
17100a								
17100b	171B	1051	A	9	H	1	66	67
17102a	171B	1051	A	9	H	1	126	127
17109b	171B	1051	A	9	H	3	36	37
17111b	171B	1051	A	9	H	3	96	97
17113d	171B	1051	A	9	H	4	6	7
17114a								
17114d	171B	1051	A	9	H	4	36	37
17115b								
17115c	171B	1051	A	9	H	4	66	67
17116b								
17116c	171B	1051	A	9	H	4	96	97

17118c	171B	1051	A	9	H	5	6	7
17120a	171B	1051	A	9	H	5	66	67
17121b	171B	1051	A	9	H	5	96	97
17123c	171B	1051	A	9	H	6	7	8
17124c	171B	1051	A	9	H	6	37	38
17124d								
17125a	171B	1051	A	9	H	6	67	68
17934c	171B	1051	A	8	H	3	6	7
17942a	171B	1051	A	8	H	4	96	97
17942b								
17943b	171B	1051	A	8	H	4	126	127
17944b	171B	1051	A	8	H	5	6	7
17947a	171B	1051	A	8	H	5	96	97
17952b	171B	1051	A	10	H	4	126	127
17954c	171B	1051	A	10	H	5	36	37
17954d	171B	1051	A	10	H	5	36	37
17955c	171B	1051	A	10	H	5	66	67
17957b	171B	1051	A	10	H	5	126	127
17957c								
17990d	171B	1051	A	10	H	1	6	7
17992d	171B	1051	A	10	H	1	66	67
17993a	171B	1051	A	10	H	1	96	97
17994a	171B	1051	A	10	H	1	126	127
17996c	171B	1051	A	10	H	2	36	37
17998c	171B	1051	A	10	H	2	96	97
17999d	171B	1051	A	10	H	2	126	127
18003a	171B	1051	A	10	H	3	96	97
18003b								
18006b	171B	1051	A	10	H	4	36	37
18013b	171B	1051	A	10	H	7	6	7
18233c	171B	1051	A	11	H	2	36	37
18244b	171B	1051	A	12	H	3	6	7
18244d								
18273a	171B	1051	A	15	H	6	66	67
18273c								
18276b	171B	1051	A	19	X	2	66	67
18280a	171B	1051	A	19	X	4	6	7
18282a	171B	1051	A	19	X	4	126	127
18703a	171B	1051	B	15	H	7	6	7
18836b	171B	1051	B	11	H	2	7	8
18839b	171B	1051	B	11	H	4	7	8
18840a	171B	1051	B	11	H	4	97	98
18841b	171B	1051	B	11	H	4	127	128
18842b	171B	1051	B	11	H	5	7	8
18847a	171B	1051	B	12	H	2	6	7
18847b								
18850b	171B	1051	B	12	H	5	6	7
18861c	171B	1051	B	17	X	3	126	127
18884a	171B	1051	A	7	H	3	66	67
18890b	171B	1051	B	7	H	5	94	95

18891b	171B	1051	B	7	H	6	5	6
18892b	171B	1051	B	7	H	6	66	67
18894c	171B	1051	B	7	H	7	35	36
18896c	171B	1051	B	8	H	1	6	7
18905c	171B	1051	B	8	H	4	96	97

Slides prepared for Witkowski et al. (2020a,b) studies:

21255d	171B	1051	A	54	X	2	5	6
21266b	171B	1051	A	58	X	1	20	21
21267d	171B	1051	A	59	X	1	20	21
21268d	171B	1051	A	60	X	1	20	21
21273c								
21273d	171B	1051	A	65	X	1	20	21
21647c	171B	1051	A	35	X	1	50	51
21658d	171B	1051	A	46	X	1	50	51
21659c	171B	1051	A	47	X	1	50	51
23789c	171B	1051	A	42	X	2	50	51
24102b	171B	1050	C	2	R	1	100	101
24103c	171B	1050	C	2	R	3	100	101
24104c	171B	1050	C	2	R	5	100	101
24556a	171B	1050	A	3	H	1	100	101
24557c	171B	1050	A	4	H	1	100	101
24558a								
24558d	171B	1050	A	6	H	1	100	101
24559a								
24559b	171B	1050	A	7	H	1	100	101
24560a	171B	1050	A	8	H	1	100	101
24561b	171B	1050	A	9	H	1	100	101
24562a	171B	1050	A	10	H	1	100	101
24563a	171B	1050	A	12	X	1	80	81
24564d	171B	1050	A	13	X	1	100	101
24565a	171B	1050	A	14	X	1	100	101
24566d	171B	1050	A	15	X	1	100	101
24567a								
24567c	171B	1050	A	16	X	1	100	101
24568b	171B	1050	A	17	X	1	100	101
24569d	171B	1050	A	18	X	1	100	101
24570d	171B	1050	A	19	X	1	80	81
24571c	171B	1050	A	20	X	1	80	81
24572d	171B	1050	A	21	X	1	80	81
24574b	171B	1050	A	23	X	1	70	71
24575b	171B	1050	A	26	X	1	100	101
24576b	171B	1050	A	27	X	1	70	71
24577c	171B	1050	A	28	X	1	90	91
24578b								
24578d	171B	1050	A	29	X	1	91	92
24579b								
24579c	171B	1050	A	30	X	1	100	101
24580b								
24580d	171B	1050	A	31	X	1	20	21
24583a	171B	1050	A	34	X	1	96	97

24584a	171B	1050	A	35	X	1	100	101
24585a	171B	1050	A	36	X	1	40	41
24585b								
24590a	171B	1051	A	2	H	2	120	121
24601a	171B	1053	A	14	H	1	50	51
24607a	171B	1053	A	20	H	1	50	51
27816a	171B	1053	A	7	H	1	50	51
27836a	171B	1051	A	57	X	1	34	35
27841a	171B	1051	A	16	H	1	6	7
27849a	171B	1051	A	20	X	5	6	7
27850a	171B	1050	A	5	H	1	100	101
27851a	171B	1051	A	25	X	1	6	7
27858a	171B	1053	A	6	H	1	50	51
27863a	171B	1051	A	18	X	1	6	7
27864a	171B	1051	A	3	H	7	5	6
27865a	171B	1050	A	11	X	1	100	101

Table 5. MRC slides of Blake Nose materials examined for this study. Abbreviations: MRC – International Ocean Discovery Program Micropaleontological Reference Center, University of Nebraska-Lincoln; H – Hole; C – Core; T – Core type; Sc – Core-section.

MRC Slide	Leg	Site	H	C	T	Sc	Interval top [cm]	Interval bottom [cm]
1050A-2H-2, 34-35 > 25 µm A	171B	1050	A	2	H	2	34	35
1050A-2H-3, 32-33 > 25 µm A	171B	1050	A	2	H	3	32	33
1050A-6H-4, 34-35 > 25 µm A	171B	1050	A	6	H	4	34	35
1050A-19X-1, 126-127 cm > 25 µm A	171B	1050	A	19	X	1	126	127
1050A-20X-1, 146-147 cm > 25 µm A	171B	1050	A	20	X	1	146	147
1050A-30X-5, 10-11 > 25 µm A	171B	1050	A	30	X	5	10	11
1050A-36X-3, 82-83 > 25 µm A	171B	1050	A	36	X	3	82	83
1050A-36X-3, 136-137 > 25 µm A	171B	1050	A	36	X	3	136	137
1050B-13X-3, 10-11 cm > 25 µm A	171B	1050	B	13	X	3	10	11
1050C-2R-1, 114-115 cm > 25 µm A	171B	1050	C	2	R	1	114	115
1053A-9H-CC > 25 µm A	171B	1053	A	9	H	CC	12	15

Table 6. SZCZ slides from deep-sea sites examined here for comparative purposes. Abbreviations: SZCZ – Institute of Marine and Environmental Sciences, University of Szczecin, Diatom Collection; H – Hole; C – Core; T – Core type; Sc – Core-section; Int. – Interval; Bot. – Bottom; USGS – United States Geological Survey; CAS – California Academy of Sciences.

SZCZ Slide	Leg	Site	H	C	T	Sc	Int. top [cm]	Int. bot. [cm]	Fraction	Comment
27585	43	386	—	15	R	3	62	63	38-63 µm	holotype of <i>Hemiaulus oreshkiniae</i>
27815	21	206	—	17	R	5	98	100	—	slide donated to SZCZ by John Barron (USGS)
27822									25-38 µm	—
27822									25-38 µm	—
27823									38-63 µm	—
27823									38-63 µm	—
27824									63-100 µm	—
27824									63-100 µm	—

27818a	1	6	—	4	R	1	57	63	—	A.L. Brigger collection split received from CAS (accession no. 610598)
27818b										
27818d										
27819a	43	386	—	15	R	3	62	63	>25 µm	—
27819b									>25 µm	—
27820b									38-63 µm	—
27821a									63-100 µm	—
27821b									63-100 µm	—

Table 7. Slides of material from onshore sites examined for this study. Abbreviations: SZCZ – Institute of Marine and Environmental Sciences, University of Szczecin, Diatom Collection; AWI – Alfred-Wegener-Institut; VSEGEI – All-Russian Geological Research Institute; BM – The Natural History Museum, London.

Slide	Site	Comment
SZCZ slides:		
27827	Kamyshlov, Sverdlovsk District, Russia	F. Hustedt sample split received from AWI (accession no. E1685)
27829	Ananino, Ulyanovsk District, Russia	S.I. Gleser sample split received from VSEGEI
BM slides:		
BM coll. Adams GC 2857	Barbados	—
BM coll. Adams H792	Barbados	—
BM 13789	Cambridge Estate, Barbados	—
BM 37876	Springfield, Barbados	—
BM 46547	Oamaru, Otago, New Zealand	—
BM 46581	Oamaru, Otago, New Zealand	—
BM 78193	D1-DODO-123 dredging, Mascarene Plateau, Indian Ocean	—

Both new slides (Table 3) and slides prepared for previous studies (Witkowski et al. 2014, 2020a, b) (Table 4) were examined in this work. For slides from previous studies, detailed information on sample processing and slide preparation techniques can be found in the relevant papers (Table 4). In addition, a number of MRC slides from Blake Nose sites (Table 5) were also examined.

Slides that were prepared specially for this study (Table 3) were made from sieved residues, cleaned following a modification of the Mandra et al. (1973) technique (Anne Gleich, Kaiser-slaubern, personal communication, 2017). Sediment soaked in a supersaturated solution of Na₂SO₄ was disaggregated by repeated freezing and thawing. After thorough washing with deionized water, the sediment underwent chemical treatment using HCl and H₂O₂. Small quantities of Na₂CO₃ and Na₄P₂O₇ were added while samples were boiling in H₂O₂. Following repeated washing in deionized water, samples were sieved through 25 µm, 38 µm, 63 µm and 100 µm sieves. 25–38 µm and 38–63 µm size fractions proved the richest in diatoms, and were used the most extensively in the present study (Tables 3 and 6).

Slides were examined using either a Zeiss AxioScope.A1 microscope, fitted with a Zeiss ICc5 digital camera and Differential Interference Contrast (DIC), or a Leica DMLB microscope equipped with a Nikon DigitalSight camera. The use of DIC is indicated in the relevant figure captions. SEM examination was performed at a number of institutions, using several devices (Hitachi S4500 at Goethe-Universität in Frankfurt am Main, JEOL JSM-6380LA at Faculty of Geology, University of Warsaw, Hitachi SU8000 at Western Pomeranian University of Technology in Szczecin).

Taxonomic Part

The taxonomic part in this work is not arranged systematically, but alphabetically by genus and species. An alphabetical rather than systematic arrangement was chosen for two reasons. First, the monophyly of numerous higher-level taxa is questioned, and second, fossil taxa are often poorly represented in diatom classifications. Instead, for each genus, a brief note on its systematic placement is given to help guide the reader. For convenience, an alphabetical list of taxa considered in this study is provided below, followed by the descriptions of taxa.

List of taxa

Taxon	Number
<i>Abas wittii</i> (Grunow) Ross & Sims	1
<i>Actinptychus heterostrophus</i> Schmidt	2
<i>Actinptychus hillabyanus</i> var. <i>corallina</i> Brun	3
<i>Actinptychus intermedius</i> Schmidt	4
<i>Actinptychus pericavatus</i> Brun	5
<i>Amphora</i> cf. <i>subpunctata</i> Grove & Sturt	6
<i>Amphora</i> cf. <i>tessellata</i> Grove & Sturt	7
<i>Amphora</i> sp. A	8
<i>Amphora</i> sp. B	9
<i>Anaulus weyprechtii</i> Grunow	10
<i>Anuloplicata ornata</i> (Grunow) Gleser	11
<i>Arachnoidiscus clarus</i> Brown	12
<i>Auliscus johnsonianus</i> Greville	13
<i>Biddulphia curvata</i> Hendey & Sims	14
<i>Biddulphia tuomeyi</i> (Bailey) Roper	15
<i>Biddulphia</i> sp. A	16
<i>Biddulphia</i> sp. B	17
<i>Briggera affixa</i> (Ross) Ross & Sims	18
<i>Briggera capitata</i> (Greville) Ross & Sims	19
<i>Briggera siberica</i> (Grunow) Ross & Sims	20
<i>Brightwellia hyperborea</i> Grunow in Van Heurck	21
<i>Brightwellia plana</i> J. Witkowski, n. sp.	22
<i>Brightwellia spiralis</i> Gleser	23
<i>Clavicula polymorpha</i> var. <i>delicatula</i> Grunow & Pantocsek	24
<i>Cortinocornus rossicus</i> (Pantocsek) Gleser	25
<i>Coscinodiscus mirabilis</i> Jousé	26
<i>Craspedodiscus ellipticus</i> Gombos	27
<i>Craspedodiscus moelleri</i> Schmidt sensu Gombos	28
<i>Craspedoporus ralfsianus</i> Greville	29
<i>Cylindrospira simsiae</i> Mitlehner	30
<i>Cymatosirid</i> morphotype A	31
<i>Cymatosirid</i> morphotype B	32
<i>Cymatosirid</i> morphotype C	33
<i>Cymatosirid</i> morphotype D	34
<i>Cymatosirid</i> morphotype E	35
<i>Cymatosirid</i> morphotype F	36
<i>Detonia wadeae</i> J. Witkowski, n. sp.	37
<i>Dextradonator eximius</i> (Grunow) Ross & Sims	38
<i>Dextradonator jeremianus</i> Ross & Sims	39
<i>Distephanosira gleichiae</i> J. Witkowski, n. sp.	40

<i>Distephanosira</i> sp. A	41
<i>Drepanotheca bivittata</i> (Grunow & Pantocsek) Schrader	42
<i>Entogonia</i> spp.	43
<i>Entogoniopsis armashevskii</i> (Pantocsek) Witkowski, Sims, Strelnikova & Williams	44
<i>Entogoniopsis dutertrei</i> (Pantocsek & Tempère) Witkowski, Sims, Strelnikova & Williams	45
<i>Entogoniopsis foveatamorpha</i> Witkowski	46
<i>Entogoniopsis polycistinora</i> (Pantocsek ex Tempère) Strelnikova, Sims, Witkowski & Williams	47
<i>Entogoniopsis venosa</i> (Brightwell) Witkowski, Sims, Strelnikova & Williams	48
<i>Eunotogramma variabile</i> Grunow	49
<i>Euodiella beatae</i> J. Witkowski, n. sp.	50
<i>Eurossia irregularis</i> (Greville) Sims var. <i>irregularis</i> Sims	51
<i>Fenneria brachiata</i> (Brightwell) Witkowski	52
<i>Fenneria kanayae</i> (Fenner) Witkowski	53
<i>Fenneria nascens</i> Brylka & Witkowski	54
<i>Grammatophora</i> spp.	55
<i>Grunowiella gemmata</i> (Grunow) Van Heurck	56
<i>Hemiaulus crenatus</i> Greville	57
<i>Hemiaulus curvataloides</i> J. Witkowski, n. sp.	58
<i>Hemiaulus imperator</i> J. Witkowski, n. sp.	59
<i>Hemiaulus inaequilaterus</i> Gombos	60
<i>Hemiaulus incurvus</i> Schibkova	61
<i>Hemiaulus jordani</i> J. Witkowski, n. sp.	62
<i>Hemiaulus lobatus</i> Greville	63
<i>Hemiaulus mesolepta</i> (Grunow) Witkowski	64
<i>Hemiaulus oreshkinae</i> J. Witkowski, n. sp.	65
<i>Hemiaulus peripterus</i> Fenner	66
<i>Hemiaulus peripterus</i> var. <i>longispinus</i> Fourtanier	67
<i>Jousea elliptica</i> (Jousé) Gleser	68
<i>Ktenodiscus aculeiferus</i> (Grunow) Blanco & Wetzel	69
<i>Ktenodiscus evermanni</i> (Hanna) Blanco & Wetzel	70
<i>Ktenodiscus kittonianus</i> (Grunow) Blanco & Wetzel	71
‘ <i>Liradiscus</i> ’ cf. <i>ellipticus</i> Greville	72
‘ <i>Liradiscus</i> ’ cf. <i>ovalis</i> Greville	73
‘ <i>Liradiscus</i> ’ sp. A	74
<i>Mastogloia rutilans</i> Brun	75
<i>Mastogloia sagitta-cupidinis</i> Brun	76
<i>Mastogloia</i> sp. A	77
<i>Medlinia abyssora</i> (Grunow) Sims	78
<i>Medlinia fenestrata</i> (Witt) Sims	79
<i>Medlinia simbirskiana</i> (Witt) Sims	80
<i>Medlinia?</i> <i>subtriangularis</i> J. Witkowski & P.A. Sims, n. sp.	81
<i>Peponia barbadensis</i> Greville	82
<i>Plagiogramma</i> sp. A	83
<i>Plagiogramma</i> sp. B	84
<i>Plagiogramma</i> sp. C	85
<i>Plagiogramma</i> sp. D	86
<i>Plagiogramma</i> sp. E	87
<i>Porpeia ornata</i> Greville	88
<i>Porpeia quadrata</i> Greville	89
<i>Proboscia ciesielskii</i> (Fenner) Witkowski	90
<i>Proboscia cretacea</i> (Hajós & Stradner) Jordan & Priddle	91
<i>Psammodiscus praenitidus</i> (Fenner) J. Witkowski, n. comb.	92

<i>Pseudopodosira aspera</i> (Jousé) Strelnikova	93
<i>Pseudopodosira bella</i> Posnova & Gleser	94
<i>Pseudopodosira jouseana</i> (Jousé) Sar, Lavigne, Wetzel, Ector & Sunesen	95
<i>Pyrgupyxis gracilis</i> (Tempère & Forti) Hendey	96
<i>Pyrgupyxis gracilis</i> var. <i>buccinalis</i> (Brun) Hendey	97
<i>Quadrocistella montana</i> Suto	98
<i>Quadrocistella paliesa</i> Suto	99
<i>Quadrocistella rectagonuma</i> Suto	100
<i>Rhaphoneis atlantica</i> Andrews	101
' <i>Rhizosolenia hebetata</i> ' Bailey sensu Homann	102
<i>Rutilaria areolata</i> Sheshukova-Poretskaya	103
<i>Rutilaria elliptica</i> Greville	104
<i>Rutilaria grevilleana</i> (Chase & Walker) Ross	105
<i>Sextiputeus inornatus</i> Ross & Sims	106
<i>Sheshukovia castellata</i> (West) Gleser	107
<i>Sheshukovia castellifera</i> (Grunow) J. Witkowski, n. comb.	108
<i>Solium exsculptum</i> Heiberg	109
<i>Stictodiscus cf. parallelus</i> (Ehrenberg) Pantocsek	110
<i>Strangulonema barbadense</i> Greville	111
<i>Thaumatonema barbadense</i> Greville	112
<i>Thaumatonema costatum</i> Greville	113
<i>Toxarium</i> sp. A	114
<i>Toxarium</i> sp. B	115
' <i>Triceratium</i> ' aff. <i>attenuatum</i> Greville	116
' <i>Triceratium</i> ' <i>blanditum</i> Greville	117
' <i>Triceratium</i> ' <i>capitatum</i> Greville	118
' <i>Triceratium</i> ' <i>exornatum</i> Greville	119
<i>Triceratium harwoodii</i> J. Witkowski, n. sp.	120
' <i>Triceratium</i> ' aff. <i>intermedium</i> Grove & Sturt	121
' <i>Triceratium</i> ' <i>kinkeri</i> Schmidt	122
' <i>Triceratium</i> ' <i>mirificum</i> Brun	123
<i>Trinacria cancellata</i> (Greville) Ross & Sims	124
<i>Trinacria cristata</i> Gombos	125
<i>Trinacria ecostata</i> Sims & Ross	126
<i>Trinacria pileolus</i> (Ehrenberg) Grunow	127
<i>Trinacria praetenuis</i> (Greville) Grunow	128
<i>Trinacria ventricosa</i> Grove & Sturt	129
<i>Trochosira cf. spinosa</i> Kitton	130
<i>Trossulus elegantulus</i> (Grove & Sturt) Ross & Sims	131
<i>Valloidiscus lanceolatus</i> Suto	132
<i>Xanthioisthmus panduraeformis</i> (Pantocsek) Suto	133
<i>Xanthiopyxis oblonga</i> Ehrenberg	134
<i>Xanthiopyxis</i> sp. sensu Fenner	135
' <i>Xanthiopyxis</i> type A' Suto	136
' <i>Xanthiopyxis</i> type B' Suto	137

I. ABAS Ross & Sims (1980)

Note: In the original description, Ross & Sims (1980) hesitated whether this genus should be classified together with hemiauloid diatoms (but see comments in Ross & Sims 1987). Subsequent workers, however, have consistently placed *Abas* within the Hemiaulaceae Heiberg (1863); see Round et al. (1990), Nikolaev & Harwood (2000, 2002) and DiatomBase (Kociolek et al. 2022).

1. *Abas wittii* (Grunow) Ross & Sims (1980), p. 120, figs 10–15

SEM: Pl. 1, Figs 1–5

LM: Pl. 2, Figs 1–9; Pl. 3, Figs 1–9

Basionym: *Syringidium wittii* Grunow in Van Heurck (1883), pl. CVI, fig. 4.

Synonym: *Syringidium poyseri* Boyer (1922), p. 9, pl. II, fig. 4.

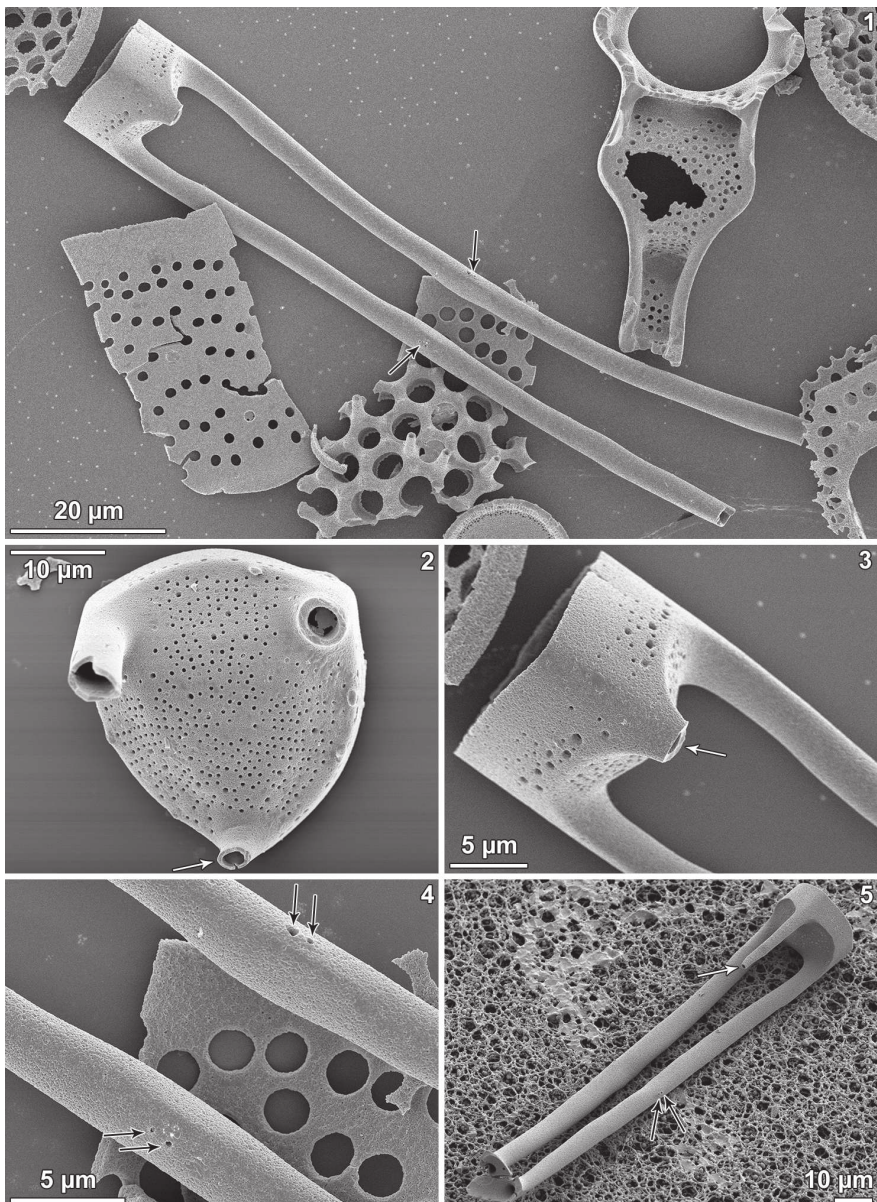
Description: Frustules subrectangular in girdle view, linked in long, straight or curved chains, with sibling valve faces located up to ~125 µm apart (Pl. 2, Fig 3–9; Pl. 3, Figs 1–9); valves tripolar (Pl. 1, Fig. 2; Pl. 2, Figs 1–2), often with minor and major axis discernible in valve view, and with convex sides, usually ~10 to 40 µm from pole to pole. Valve face domed, with fine poroid areolae arranged in radial rows (Pl. 1, Fig. 2; Pl. 2, Figs 1–2). Tubular hyaline polar elevations are located at two poles (Pl. 1, Figs 1–5; Pl. 2, Figs 1–9; Pl. 3, Figs 1–9). Projecting from the third pole is a spear-shaped process (terminology from Ross & Sims 1980) (Pl. 1, Figs 2–3, 5; Pl. 2, Figs 1, 5, 7; Pl. 3, Figs 2, 6–9). The tubular polar elevations are fused with those of the sibling (Pl. 1, Figs 1, 4–5; Pl. 2, Figs 3–9; Pl. 3, Figs 3–5). The fused polar elevations may be deflected toward one another, occasionally meeting or even fusing at about half-way between the siblings (Pl. 3, Figs 6–9). Mantle clearly differentiated from the valve face, vertical and deep (Pl. 2, Figs 3–5; Pl. 3, Figs 4–9). Mantle areolae (7 in 10 µm) sometimes form distinct rows parallel to the pervalvar axis (Pl. 2, Figs 3–5), but on some valves the mantle is largely hyaline, with only a narrow band of perforations below the valve face-mantle junction (Pl. 1, Fig. 3). Valvocopulae often preserved, extremely deep, but exact girdle band structure unresolved (Pl. 3, Figs 1–2, 4–9) (see Ross & Sims 1980, for further details of the girdle structure).

Occurrence (this study): At Site 1050, *A. wittii* is observed discontinuously from Core 1050A-26X (238.62 cmbsf sub-bottom depth; Magnetozone C24r, lower Eocene) to the top of Hole, within Magnetozone C19r (middle Eocene) (Text-fig. 2). At Site 1051, *A. wittii* also occurs discontinuously from Core 1051A-47X (524.83 cmbsf; Magnetozone C24n, lower Eocene) to the top of Hole, within Magnetozone C17n in the lower upper Eocene (Text-fig. 2).

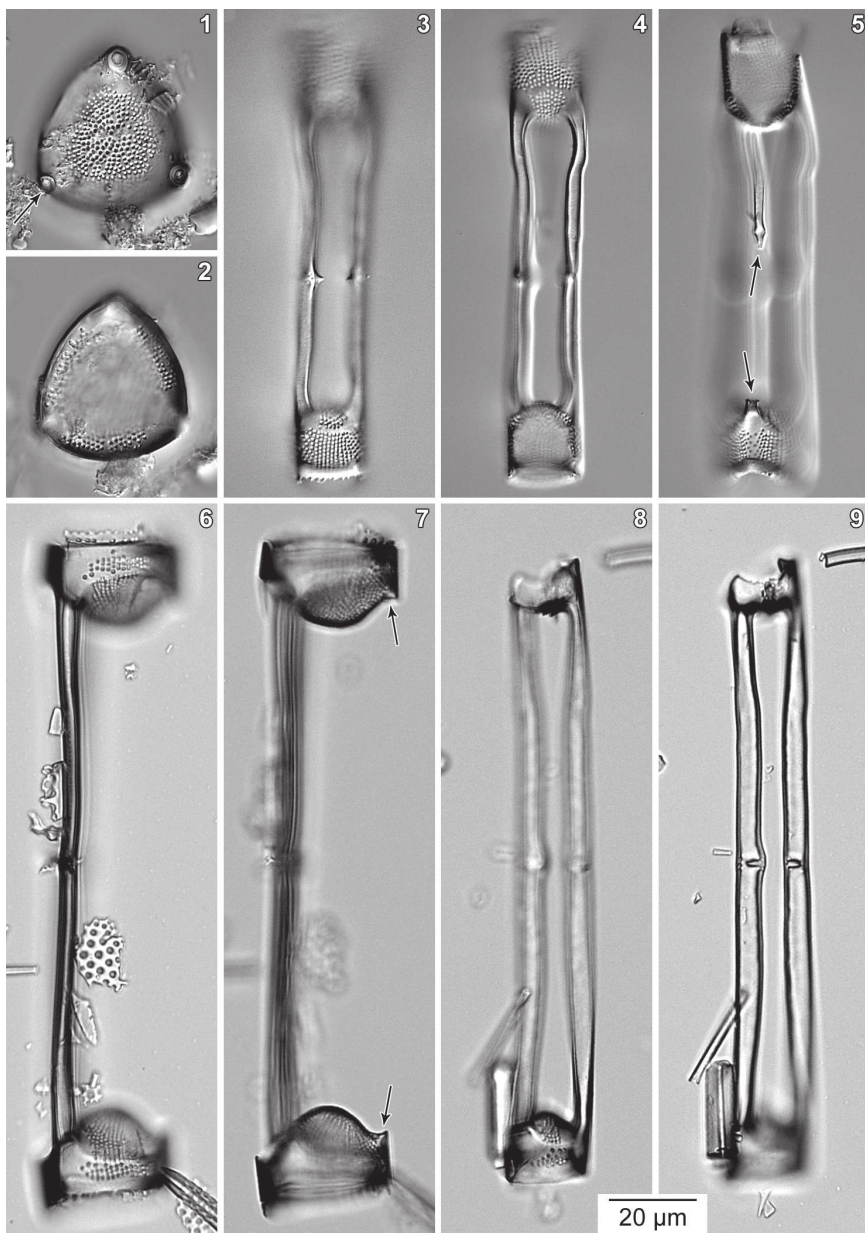
Discussion: Because of its extremely long pervalvar axis (Pl. 2, Figs 6–9; Pl. 3, Figs 1–9), *A. wittii* is seldom seen in valve view. Specimens that are positioned in valve view in strewn slides (Pl. 1, Fig. 2; Pl. 2, Figs 1–2), have all projections broken off, and are thus easily confused with other, less common tripolar taxa.

As discussed in Ross & Sims (1980) and Round et al. (1990), *Abas* is one of the few examples of fusing as a linking mechanism in diatoms. The junction between the polar elevations of siblings is clearly visible in LM, but not in SEM, where a seemingly featureless tube is seen extending between valves of adjacent cells (Pl. 1, Figs 1, 4–5; Pl. 2, Figs 3–9; Pl. 3, Figs 1–9). SEM examination reveals that the probable junction is often slightly inflated and bears a pair of small openings (Pl. 1, Figs 1, 4–5). LM observations indicate that the actual junction lies probably in between these perforations.

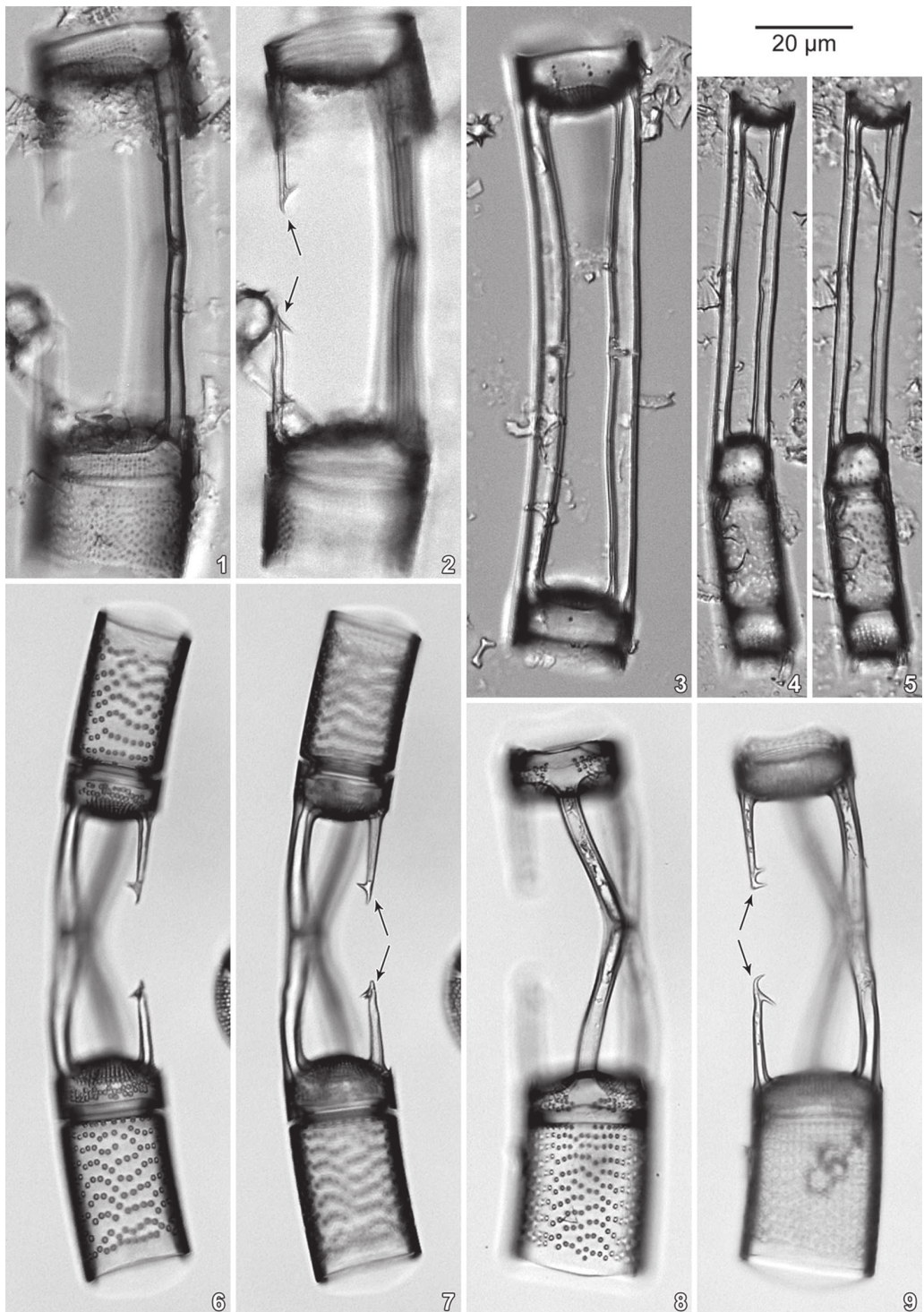
Most published records document *A. wittii* from middle Eocene successions. In this study, however, the occurrences of *A. wittii* are spotty and therefore downworking and any possible labora-

**Plate 1**

Scanning electron micrographs of *Abas wittii* (Boyer) Ross & Sims. Specimens in Figs 1, 3 and 4 from sample ODP 171B-1050A-21X-2, 100–101 cm. Specimen in Fig. 2 from sample ODP 171B-1050A-3H-6, 100–101 cm. Specimen in Fig. 5 from sample ODP 171B-1051B-8H-5, 5–6 cm. Fig. 1. Flat external view of a valve with long polar elevations preserved. Arrows indicate the approximate point of fusion between polar elevations of sibling valves. Fig. 2. Oblique valve view. Both the polar elevations and the spear-shaped process are broken off. White arrow indicates the position of the spear-shaped process, distinguished by the smaller diameter in comparison to the polar elevations. Fig. 3. Detail of the specimen in Fig. 1, showing the sparse mantle areolation. White arrow points to the base of the broken spear-shaped process. Fig. 4. Detail of the specimen in Fig. 1, showing the slightly inflated fused portions of the polar elevations from both siblings. Note the pairs of openings indicated by black arrows, presumably one to each polar elevation. Fig. 5. Oblique external view of a valve with prominent polar elevations still fused with those of the sibling, even though the sibling valve is broken off. White arrow indicates the spear-shaped process, with the tip broken off.

**Plate 2**

Light micrographs showing the range of morphological variation in *Abas wittii* (Boyer) Ross & Sims. Each pair or triplet (Figs 3–5) of micrographs shows the same specimen at various focal levels. Specimen in Figs 1–2 from sample ODP 171B-1051A-8H-3, 6–7 cm. Specimens in Figs 3–9 from sample ODP 171B-1050A-3H-6, 100–101 cm. Figs 1–2. Valve view of a specimen with both the polar elevations and the spear-shaped process (arrow) broken off. Photographed using DIC. Slide SZCZ 17934c. Figs 3–5. Focus-through series of a pair of small, linked siblings. Black arrows in Fig. 5 point to the preserved spear-shaped process on the upper sibling, and the base of a broken process on the lower sibling. Photographed using DIC. Slide SZCZ 27831b. Figs 6–7. Pair of large siblings with exceptionally long and slender polar elevations. Note the polar elevations are aligned with one another and therefore it appears as though only one is preserved. Black arrows point to the positions of the spear-shaped processes, which are missing on both valves. Slide SZCZ 27832b. Figs 8–9. Pair of narrow siblings with strongly expanded polar elevations. Slide SZCZ 27832b.



tory contamination are difficult to distinguish from in situ occurrences. *Abas wittii* appears to be broadly distributed in mid-latitude middle Eocene successions, and should be investigated as a likely biostratigraphic marker in future studies. The top of the stratigraphic range of *A. wittii* is poorly constrained due to the poor age control available for the Barbados deposits (for references on age control uncertainties see Witkowski et al. 2015, p. 5), from which it was originally proposed. There are no reliably dated occurrences of *A. wittii* younger than the late Eocene in ODP Hole 1053A.

Ross & Sims (1980) considered *A. wittii* as closely related to *Dextradonator jeremianus* Ross & Sims (see #39, below), based on similarities in girdle structure. In Round et al. (1990) and Nikolaev & Harwood (2002), both *Abas* and *Dextradonator* are placed within the Family Hemiaulaceae Heiberg (1863). Stratigraphic data do suggest *Abas* and *Dextradonator* may have evolved at a similar time, as both these taxa have their first occurrences at correlative levels in Holes 1050A and 1051A. If that is the case, however, their common ancestor remains unknown. Like bi- and multipolar hemiauloids, represented by *Hemiaulus* Heiberg and *Trinacria* Heiberg, respectively, *Abas* has poroid valve structure. Unlike these typical Hemiaulaceae, however, elevations in *Abas* are present at only two poles, the third being occupied by the prominent spear-shaped process, which likely represents a modified rimoportula. Further, the sibling valves of *Abas* are fused with one another, in contrast to most genera of the Hemiaulaceae, which use linking spines to join their cells in chains. Thus, whether or not *Abas* should be classified together with bipolar hemiauloid diatoms, remains a matter of debate.

Geographic and stratigraphic distribution in published records:

Middle Eocene:

DSDP Hole 390A, Blake Nose, western North Atlantic: Fenner (1985), p. 727, fig. 10.4 (as *Abas wittii* (Grunow) Ross & Sims).

DSDP Hole 605, North American continental margin, western North Atlantic: Gombos (1987), tab. 3 (as *Abas wittii*).

ODP Hole 707C, Mascarene Plateau, Chagos Ridge, Western Indian Ocean: Fenner & Mikkelsen (1990), p. 440, tab. 3 (as *Abas wittii* (Grunow) Ross & Sims).

ODP Site 1051, Blake Nose, western North Atlantic: Witkowski et al. (2014), tab. 1, pl. I, figs 11a–b (as *Abas wittii*).

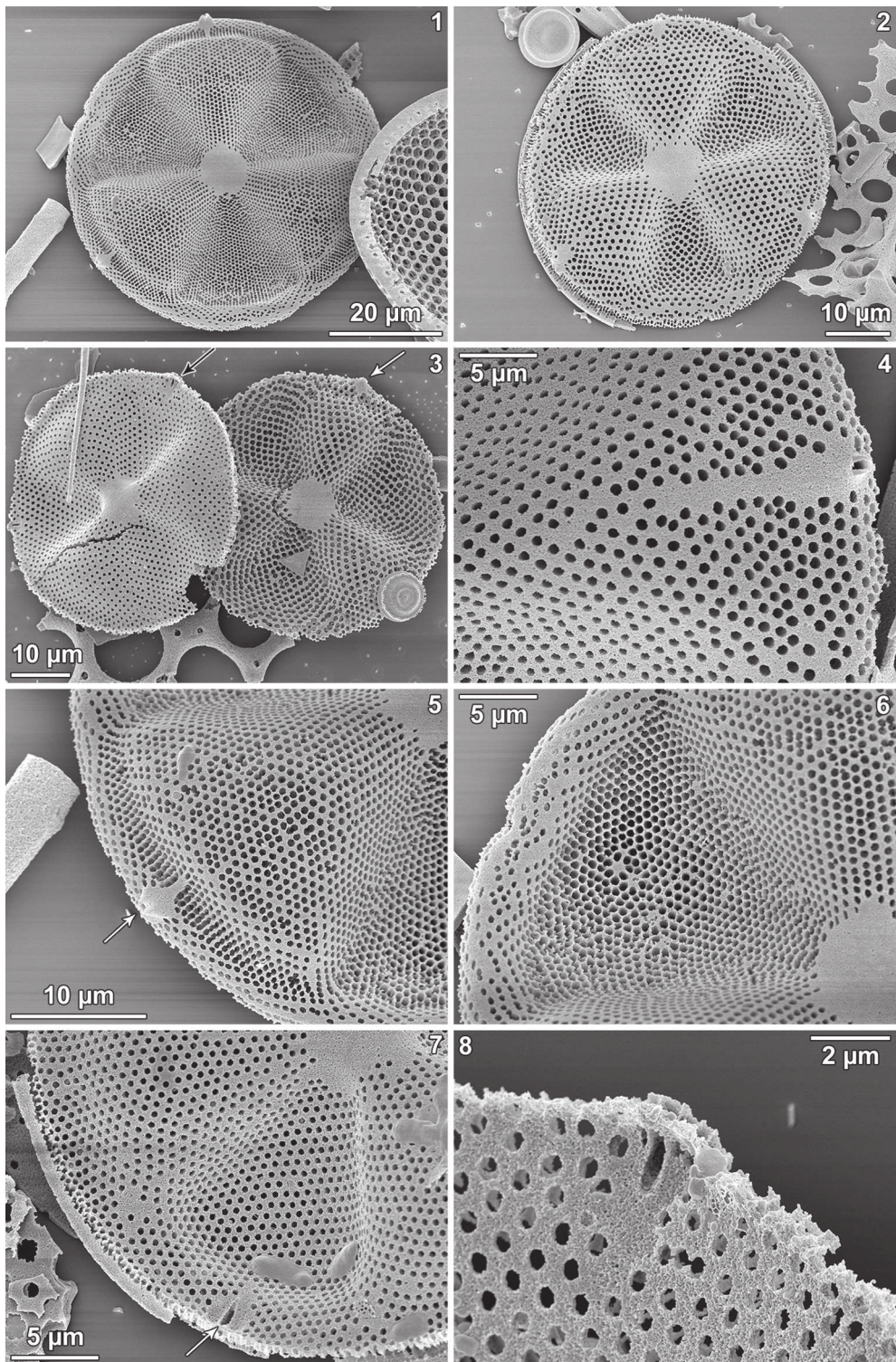
ODP Holes 1050A and 1051A, Blake Nose, western North Atlantic: Witkowski et al. (2020a), pl. I, fig. 9 (as *Abas wittii* (Grunow) Ross & Sims).

Middle to upper Eocene (age assignment from Ross & Sims 1980):

DODO-123-D-1 dredging, Mascarene Plateau, Western Indian Ocean: Ross & Sims (1980), p. 120, figs 10–15 (as *Abas wittii* (Grunow) Ross & Sims).

Plate 3

Light micrographs showing the range of morphological variation in *Abas wittii* (Boyer) Ross & Sims. Each pair of micrographs, except for Fig. 3, shows high and low focus of the same specimen. Specimen in Figs 1–2 from sample ODP 171B-1051A-8H-4, 126–127 cm. Specimen in Fig. 3 from sample ODP 171B-1051A-8H-1, 16–17 cm. Specimen in Figs 4–5 from sample ODP 171B-1051A-8H-1, 26–27 cm. Specimens in Figs 6–9 from D1-DODO-123 dredging, Mascarene Plateau, Indian Ocean. Figs 1–2. Linked sibling valves, lower valve with valvocopula attached. Note the spear-shaped processes on the left-hand sides of both valves (arrows in Fig. 2). Slide SZCZ 17943b. Fig. 3. Linked sibling valves. Note the hyaline polar elevations do not come in close proximity. Slide SZCZ 17091b. Figs 4–5. A frustule (bottom) with an attached sibling valve (top). Note the hyaline polar elevations do not come in close proximity. Slide SZCZ 17091b. Figs 6–7. Linked sibling valves, both with valvocopulae attached. Note spear-shaped processes on the right-hand sides of both valves (arrows). Also note that the hyaline polar elevations curve strongly inward. The Slide BM 78193. Figs 8–9. Linked sibling valves, lower valve with valvocopula attached. Note the spear-shaped processes on the left-hand sides of both valves (arrows). Also note that the hyaline polar elevations curve strongly inward. Slide BM 78193.



Middle Eocene-lower Miocene(?):

Cambridge Estate, Barbados: Van Heurck (1883), pl. CVI, fig. 4 (as *Syringidium wittii* Grunow).
Barbados: Boyer (1922), p. 9, pl. II, fig. 4 (as *Syringidium poyseri* Boyer); Hustedt (1940), taf. 434, figs 11–12 (as *Syringidium poyseri* Boyer).

Eocene-Oligocene (age assignment from Round et al. 1990):

no sites specified, presumably DODO-123-D-1: Round et al. (1990), p. 270, figs a–g.

II. *ACTINOPTYCHUS* Ehrenberg (1843)

Note: *Actinoptychus* is a common surf-zone diatom, living attached to sand grains (Round et al. 1990). The presence of numerous species of this genus in deep-sea sediments cored at Blake Nose is thought to result from sustained offshore export of neritic diatoms from the North American continental margin through the Paleocene and Eocene period (see related notes under #6, *Amphora* cf. *subpunctata*, #11, *Anuloplicata ornata*, #12, *Arachnoidiscus clarus*, #93–95, *Pseudopodosira* spp., etc.). For an extended discussion on this issue, see Witkowski et al. (2014; 2020b).

Together with other genera bearing radial raised and depressed sectors on the valve face, *Actinoptychus* is classified within the Family Heliopeltaceae Smith (1872) – see Ross & Sims (1973, 1997, 2002), Simonsen (1979), Gleser et al. (1988), Round et al. (1990), Nikolaev & Harwood (2000, 2002).

2. *Actinoptychus heterostrophus* Schmidt (1875), taf. 29, fig. 2

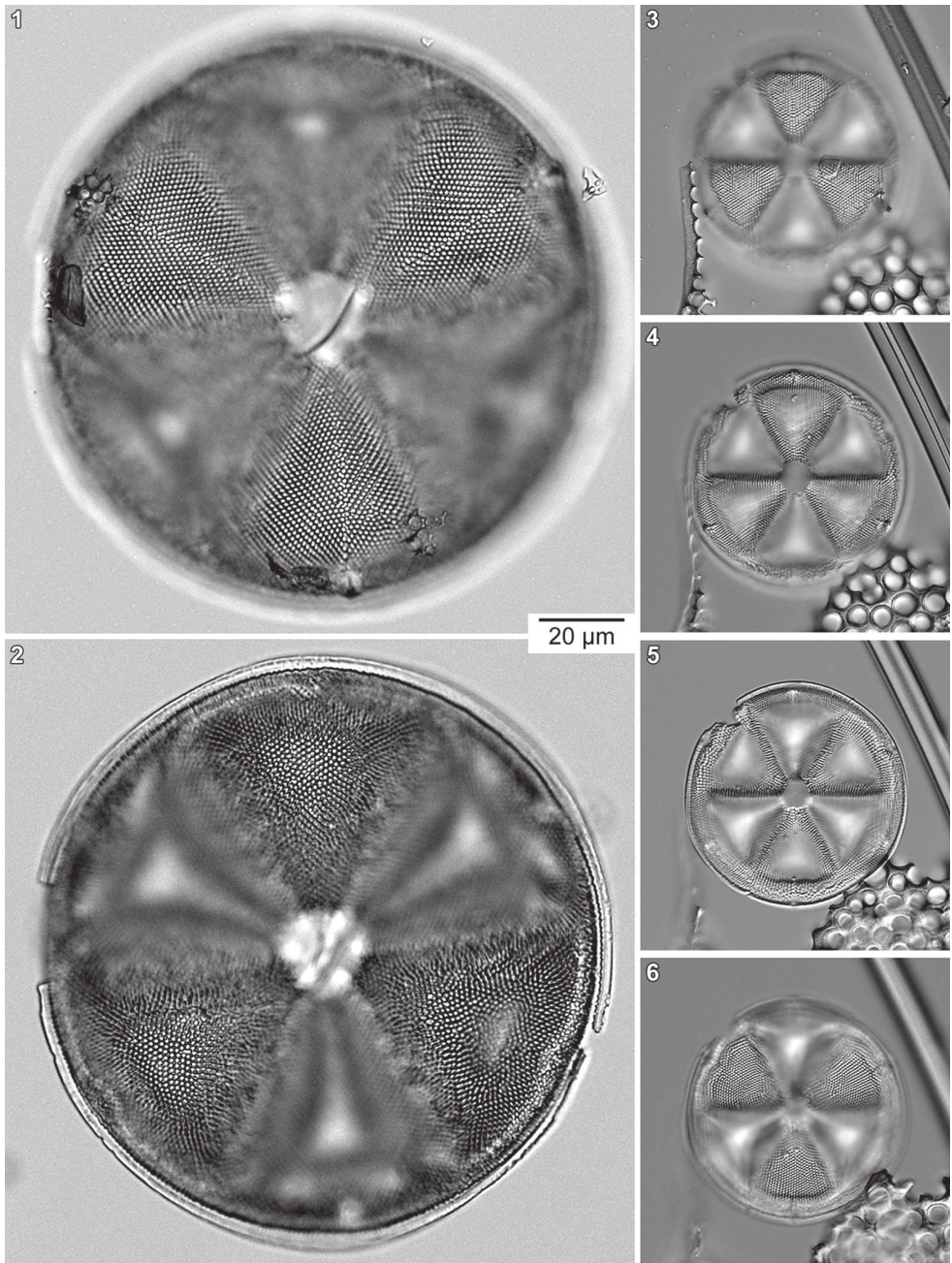
SEM: Pl. 4, Figs 1–8

LM: Pl. 5, Figs 1–6

Description: Valves circular, ~50–130 µm in diameter, strongly undulate (Pl. 4, Figs 1–3), divided into six alternating raised and depressed sectors radiating from a small, hexagonal hyaline central area (Pl. 4, Figs 1–3, Pl. 5, Figs 1–6). The distal edges of the raised sectors are distinctly cut off from the broad valve face margin (Pl. 4, Figs 1–2, 5, 7; Pl. 5, Figs 3–6). Except for the small hyaline central area, whole valve face is perforated by poroid areolae (Pl. 4, Figs 1–8; Pl.

Plate 4

Scanning electron micrographs of *Actinoptychus heterostrophus* Schmidt. All specimens from sample ODP 171B-1050C-2R-5, 100–101 cm. Fig. 1. Flat external view of a specimen with the mantle margin broken off. Note the absence of radial hyaline bands within the distal parts of the raised sectors. Fig. 2. Oblique external view of a valve with partly preserved mantle margin. Note the presence of short, radial hyaline bands within the distal parts of the raised sectors. Fig. 3. Probably a disarticulated pair of complementary sibling valves. Oblique internal view on the left and flat external view on the right. Note the small valve of *Pseudopodosira bella* attached in the lower right corner. External and internal openings to the rimoportulae indicated by white and black arrow, respectively. Fig. 4. Detail of a raised sector, showing a broken tube positioned within a small hyaline area that grades into a narrow hyaline band pointing toward the valve face center. Fig. 5. Detail of a raised sector, showing the distal edge, cut off next to the external tube of a rimoportula (arrow). Note the absence of a radial hyaline band within the distal part of the raised sector. Fig. 6. Detail of a depressed sector. Note the densely packed areolae within the sector, and less densely distributed areolae closer to the distal edge of the depressed sector. Fig. 7. Detail of valve interior, showing a partly preserved mantle margin. Arrow indicates the internal opening of a rimoportula. Note the distal edge of the raised sector, visible immediately above the rimoportula opening. Fig. 8. Detail of valve interior, showing an internal opening to a rimoportula in the form of a short, straight slit. Note the fracture through the valve, revealing a poroid valve structure.

**Plate 5**

Light micrographs of *Actinoptychus heterostrophus* Schmidt. Each column shows the same specimen in valve view at various focal levels. All specimens from sample ODP 171B-1050C-2R-5, 100–101 cm. Figs 1–2. Large valve with radial hyaline bands extending through nearly the whole axes of the raised sectors. Slide SZCZ 27834a. Figs 3–6. Mid-sized valve lacking hyaline bands within the raised sectors, photographed using DIC. Note the cut off distal edges of the raised sectors in Figs 3 and 4. Slide SZCZ 27833a.

5, Figs 1–6). Within raised sectors, areolae are aligned in parallel, decussate rows and are less densely packed (9 areolae in 10 µm) than areolae within depressed sectors (Pl. 4, Figs 2, 5–7). Areolation density within depressed sectors also decreases closer to the valve face margin. At the valve face-mantle transition, a short distance from the distal edges of the raised sectors, there are three short hyaline tubes, often positioned within a small, linear, radially aligned hyaline area (Pl. 4, Figs 1–5). These tubes represent external openings to the rimoportulae. Mantle shallow, densely areolated (Pl. 4, Figs 2, 7). Valve interior reveals short, straight, radially aligned slits at the valve face-mantle transition, which represent internal openings to the rimoportulae (Pl. 4, Figs 7–8). At the free edge of the mantle, there is a narrow, hyaline margin (Pl. 4, Figs 2, 7; Pl. 5, Fig. 2).

Discussion: The diagnostic features of *A. heterostrophus* include the conspicuously cut-off distal edges of the raised sectors (Pl. 4, Figs 1–2, 5; Pl. 5, Figs 3–6), and the decrease in areolation density toward the distal edges of the depressed sectors (Pl. 4, Figs 2, 6). There is also one feature that displays some variation. The rimoportulae are positioned within small, irregular hyaline areas. These may be elongated to form narrow, linear, radially aligned bands projecting toward the valve face center. In the Blake Nose cores, these were never found to reach to the valve face center. Instead, they terminate mid-way through the axis of the raised sector (Pl. 4, Figs 1–2, 4; Pl. 5, Fig. 1).

The specimens of *A. heterostrophus* examined here are only moderately preserved. For scanning electron micrographs of well-preserved material, see Strelnikova (1995), who illustrated specimens with nearly complete mantle margins (Strelnikova 1995, fig. 1) and with partially preserved cribra (fig. 2 in Strelnikova 1995). The valve morphology, however, is consistent between the specimens from the Blake Nose cores and from Russian sites. This makes *A. heterostrophus* one of the many taxa included in the present study that are common to mid-latitude North Atlantic and Eurasian Platform sites (see also comments in Witkowski et al. 2020a).

Occurrence (this study): At Site 1050, *A. heterostrophus* was observed from Core 1050C-2R (333.89 cmbsf sub-bottom depth; upper Magnetozone C27n, upper lower Paleocene) through Core 1050A-35X (305.89 cmbsf; middle Magnetozone C26r, middle Paleocene) (Text-fig. 2). At Site 1051, *A. heterostrophus* was observed only in Core 1051A-63X (572.70 cmbsf; probably within Magnetozone C26r, middle Paleocene) (Text-fig. 2).

Geographic and stratigraphic distribution in published records:

Senonian (Upper Cretaceous):

Gulf of Gdańsk coast, Poland: Schulz (1935), p. 385 (as *Actinoptychus heterostrophus* Schmidt).

Upper Campanian (Upper Cretaceous):

Severnaya Sos'va River, Russia: Strelnikova (1974), p. 69, pl. XIV, fig. 8 (as *Actinoptychus heterostrophus* Schmidt).

Til'tim, Synya River basin, Russia: Strelnikova (1995), p. 433, fig. 4; Strelnikova & Tsoy (2008), p. 60, pl. 72, fig. 5 (as *Actinoptychus heterostrophus* Schmidt).

Upper Cretaceous:

Eastern slopes of Urals, Russia: Strelnikova & Tsoy (2008), p. 60, pl. 71, figs 1–3 (as *Actinoptychus heterostrophus* Schmidt).

Paleocene:

Inza and Sengiley, Ulyanovsk District, Russia: Strelnikova (1995), p. 433, figs 1–3, 5–6 (as *Actinoptychus heterostrophus* Schmidt); Strelnikova & Tsoy (2008), p. 60, pl. 72, figs 1–3, 4, 6–8 (as *Actinoptychus heterostrophus* Schmidt).